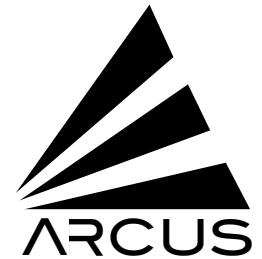


MIT Kavli Institute



MEMORANDUM

November 16, 2017

To: *Arcus* Simulations & Calibration Team
From: David P. Huenemoerder
Subject: Technical Note: Background estimate: scaling the *Chandra*/HETGS Background Rate to *Arcus*
Revision: 1.0
URL: http://space.mit.edu/home/dph/arcus/background_hetg_scaling.pdf
File: background_hetg_scaling.tex

1 Overview

We can use the *Chandra*/HETGS background to estimate a similar contribution to the *Arcus* background. Details for the HETGS analysis can be found at http://space.mit.edu/cxc/docs/hetg_bg. The main conclusion of that study was that the dominant source of background (extracted in long exposures of faint or heavily absorbed sources, but from off-source spatial regions) is from charged particles (presumed to be high energy protons) interacting with the CCDs. The rate did not depend on Galactic latitude, but did depend on time, in anti-correlation with the solar cycle. Hence, we can use these data, under the assumptions of a similar radiation environment of high orbits for *Arcus* and *Chandra*, and of similar back-illuminated (BI) CCD detectors, with the caveat that there may be differences in detector shielding.

1.1 The HETG Background

It is instructive to examine the spatial-spectral distribution of the ACIS/HETG counts. Figure 1 shows an intensity image of the CCD energy vs dispersion, accumulated from the MEG spatial regions from off-source extractions in 6 observations, with over 800 ks exposure, after removal of bad events (known to be non-X-ray). The ACIS spectroscopic array (ACIS-S) has 6 CCDs, denoted by S0 to S5. S1 and S3 are BI devices and stand out with higher background rates.

Two of the observations had heavily absorbed, but high-energy-bright sources in the field, whose dispersed spectra crossed the MEG background spatial region. These show as hyperbolic segments labeled “interloper sources”.

Below these, around 2 keV, are horizontally distributed enhancements. These are due to fluorescence of gold M-shell α and β lines in the CCD frame-store filter (upper band) and from Si $K\alpha$ in the CCD (lower,

brighter band). Some of the Si K is also due to the excitation by the bright source’s photons, but since the distribution spans the entire array, it is also from background (e.g., nearly as strong on S1 as S3).

At the lowest energies, there is enhanced background at the limit of the CCD event detection threshold.

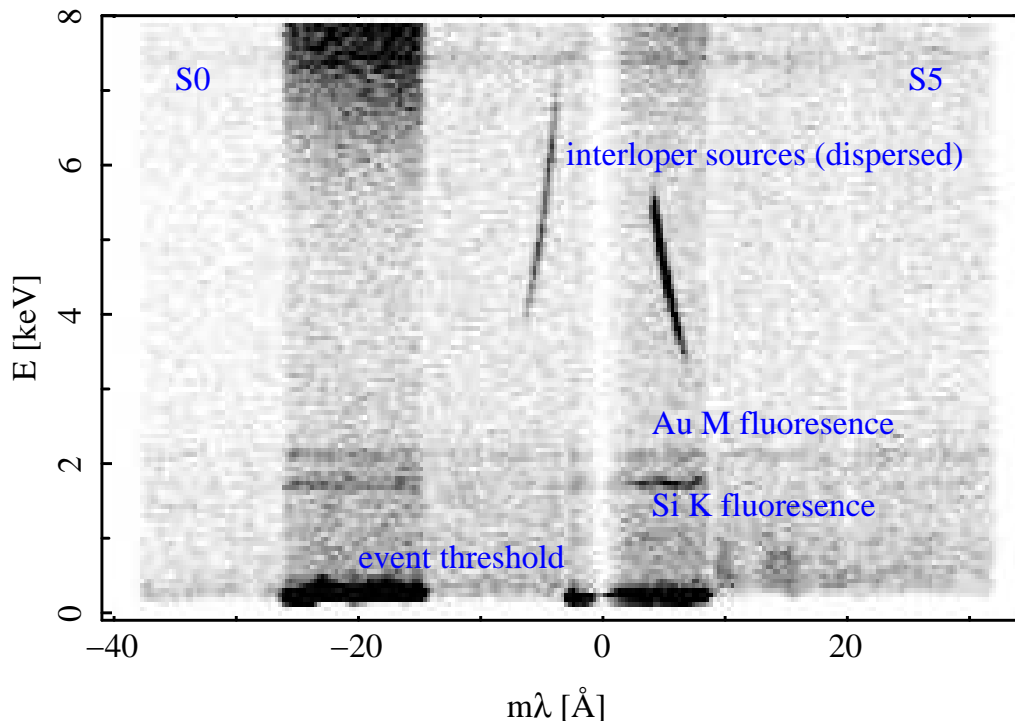


Figure 1 – MEG background data for off-source extractions accumulated from 6 observations and about 800 ks. The y -axis is the CCD “smeared” energy, after applying gain and CTI corrections to the PHA values. The x -axis is the high-resolution dispersion coordinate along the orders. “S0” and “S5” label the outer CCDs, which run sequentially from left to right; S1 and S3 are back-illuminated devices. “Interloper...” is from the sources in two of the observations whose dispersed spectra cross the background spatial region. Gold and silicon fluorescence in the detector are visible as horizontal bands near 2 keV. Background is enhanced on the BI CCDs near the event detection threshold.

The CCD energy and CCD response are used to order-sort dispersed spectra, since at any dispersion location, we know what the energy should be, and that events have a distribution defined by the CCD response at that energy. Hence, we can “flatten” the dispersed spectra (hyperbolas) by dividing the grating $m\lambda$ value by the CCD “ λ ” (hc/E). Figure 2 shows the same data from Figure 1 thus transformed into a real-valued dispersion order on the y -axis; at any $m\lambda$, order is still proportional to energy. In the top plot, we can see that the interloper source is well separated from first order and that there is no obvious first-order signal (which would be a strong horizontal distribution centered on $m = 1$). The constant energy fluorescent features are now diagonal stripes (higher energy has higher slope; the inner empty cone represents the high-energy cutoff of the dispersed spectral region at 1 \AA (12 keV)).

The bottom plot shows an expanded range around first order. The gray box is an approximate bounding rectangle for first order (the actual implemented region follows contours of the energy- and position-dependent CCD responses which enclose 90–95% of the energy fraction).

The extracted background spectrum is shown in Figure 3 (where the HEG part, not shown until now,

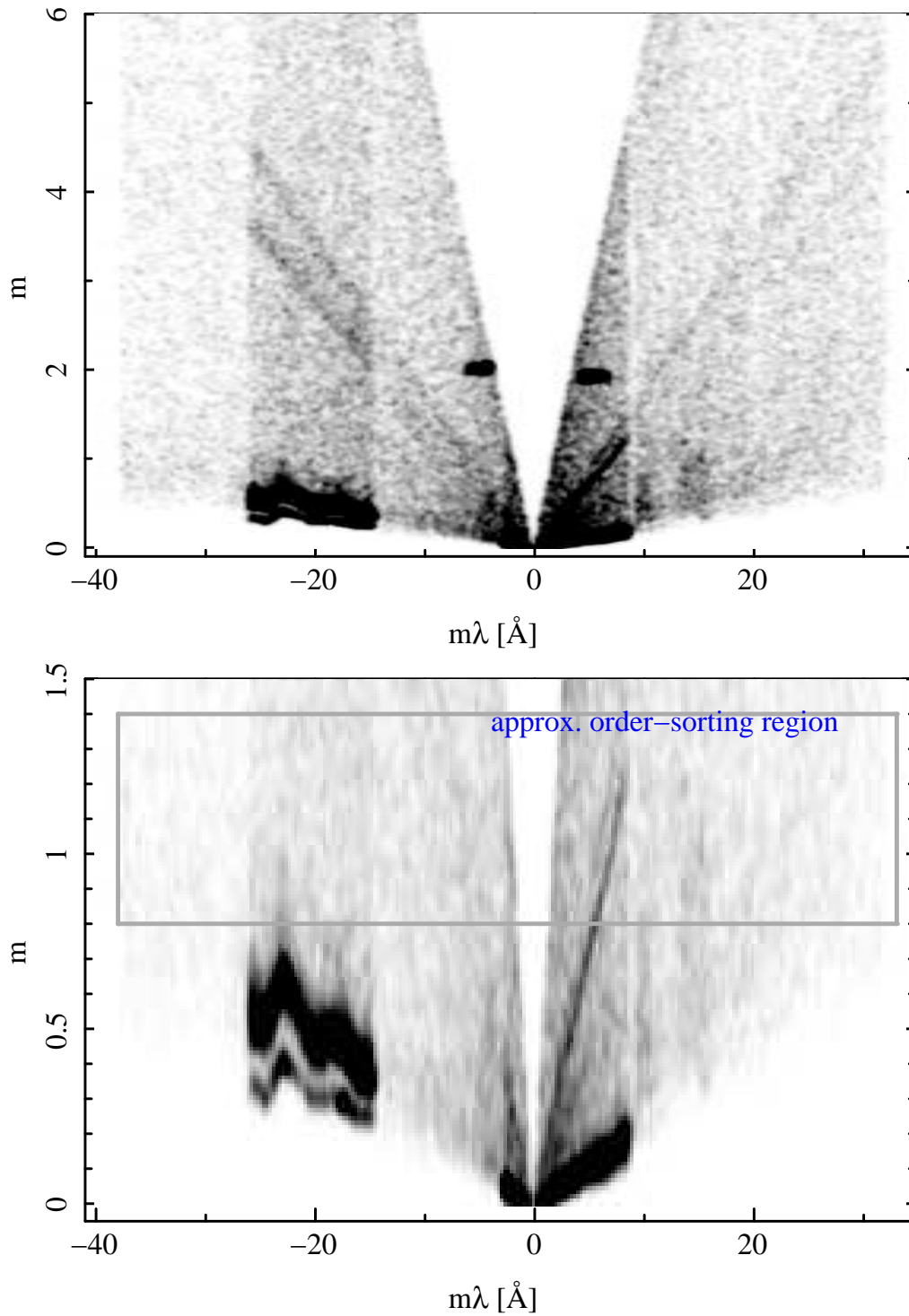


Figure 2 – MEG background data, vs order. This is the same data shown in Figure 1, but with the energy transformed into the real-valued diffraction order. The bottom panel is an expanded range about first order.

is also included). We can identify most of the features with the those in the prior figures, namely the fluorescent peak near $+7 \text{ \AA}$ (it's much weaker on the FI CCD in negative order), the spike near -24 \AA which is background from near the event detection threshold. The spike near $+15 \text{ \AA}$ seems to be noise, and is visible as a weak enhancement in Figure 2, bottom panel.

The BI rate near 20 \AA is about $0.5 \text{ counts/Ms}/\text{FWHM}/4 \text{ arcsec}$, where the latter factor is due to the 4 arcsec spatial extraction width. Implicit here is the extraction region in the order sorting dimension (energy), which at $m\lambda \sim -20$ is about 225 eV .

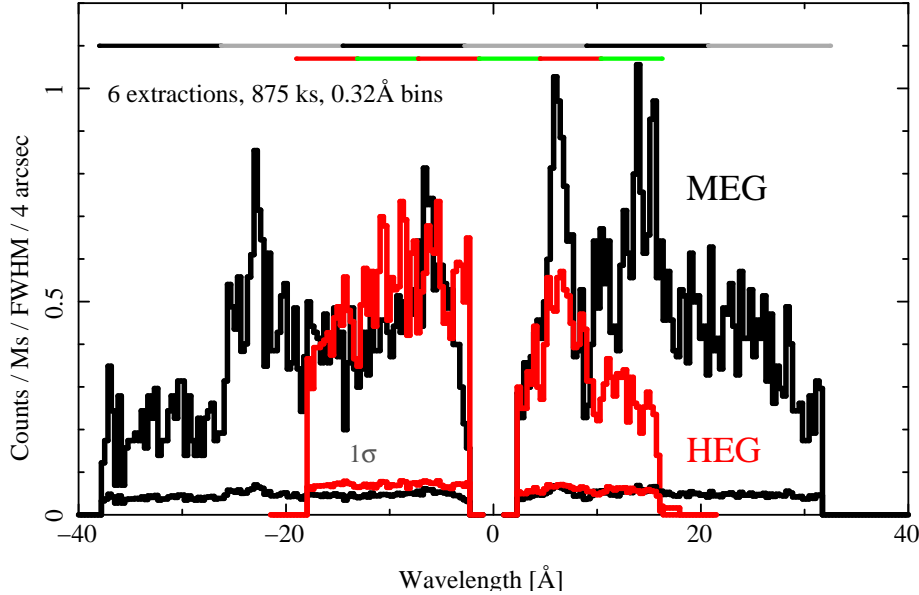


Figure 3 – The first orders’ HETG count rate density, scaled to the FWHM in the dispersion direction and the default cross-dispersion extraction width for HEG (red) and MEG (black). The 1σ counting statistics uncertainty level is shown at the bottom of the plot. The approximate locations of each CCD are shown by the alternating color bars for MEG (upper) and HEG (lower), from S0 (leftmost) to S5.

2 Transfer to *Arcus*

The above-derived HETGS rate represents an approximately uniform count rate per pixel per extraction cell due to high energy particles, and not celestial X-rays. We can scale this from the HETGS detection cell to that of *Arcus*, assuming all other conditions are identical, for energies below about 2 keV as apropos of *Arcus* (and where the strong fluorescent features are not present). We can also convert this to a background “PHA” file for use in simulations.

The HETGS extraction cell is about 15 square pixels with a 225 eV window, which leads to a background rate of $\sim 1.2 \times 10^{-10} \text{ counts/pixel}^2/\text{s/eV}$.

The *Arcus* order-sorting space is full, unlike that of HETGS. This does not increase the background per order, but does make determination of the inter-order background rely on spatially separate off-source extraction regions, or on blank-field pointings. In Figure 4 we show a representative model order-sorting plot using a CCD redistribution model with a 70 eV Gaussian FWHM at 20 \AA . For $m = 6$ at 22 \AA , ($m\lambda = 132 \text{ \AA}$), the order full width is about $\pm 30\%$, or about 340 eV .

An *Arcus* spatial extraction cell is about $12 \times 50 \text{ pix}^2$ (dispersion FWHM \times cross dispersion), with $24 \mu\text{m}$ pixels (similar to *Chandra/ACIS*). This yields a background rate of $\sim 2.4 \times 10^{-5}$ counts/s/cell. Assuming that this is for a resolving power of $R = 2500$, the rate density is 2.7×10^{-3} counts/s/ \AA in the critical region.

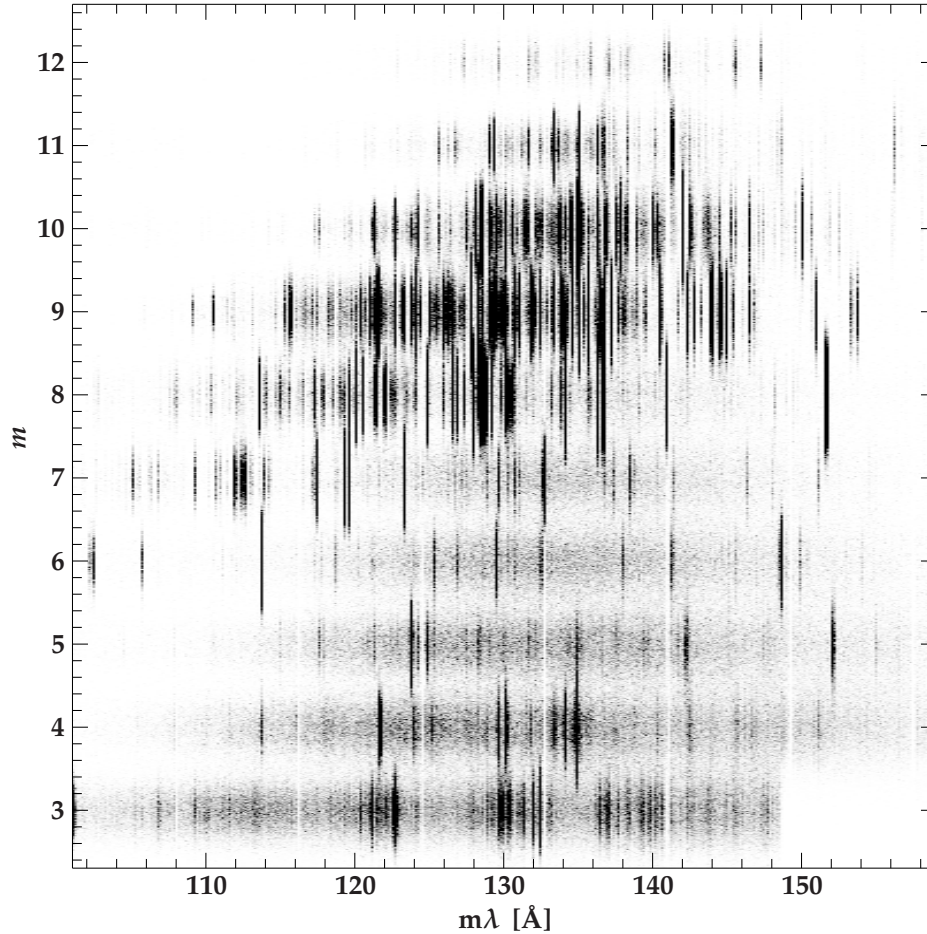


Figure 4 – *Arcus* simulated order-sorting (Nov 2016 raytrace and CCD model version). In the region of primary interest, 22 \AA in order 6 ($m\lambda = 132 \text{ \AA}$), the order-sorting width is about ± 0.3 orders, or 340 eV .

3 Summary

The relevant number for estimating *Arcus* charged-particle background, as scaled from *Chandra/HETGS*, is 1.2×10^{-10} counts/pixel²/s/eV. For typical cross-dispersion and order-sorting regions, this can be scaled by $50 \text{ pixels} \times 340 \text{ eV}$, to $2 \text{ counts/Ms/pixel}$ in an extracted spectrum.

A Background "PHA" File

TBS. (i.e., counts per bin per order for some large exposure, with a backscale of 1.0, not to be folded through the response, but to be scaled and added to simulated counts).